

## ARTICLE

# A new ratiometric switch “two-way” detects hydrazine and hypochlorite via “dye-release” mechanism with PBMCs bioimaging study

Received 00th January 20xx,  
Accepted 00th January 20xx

DOI: 10.1039/x0xx00000x

Sangita Das,<sup>a,b,c,\*</sup> Lakshman Patra,<sup>a</sup> Partha Pratim Das<sup>d</sup>, Kakali Ghoshal,<sup>e</sup> Saswati Gharami,<sup>a</sup> James. W. Walton,<sup>b</sup> Maitree Bhattacharyya<sup>e</sup> and Tapan Kumar Mondal<sup>a,\*</sup>

A new ratiometric fluorescent probe (*E*)-2-(benzo[d]thiazol-2-yl)-3-(8-methoxyquinolin-2-yl)acrylonitrile (**HQCN**) has been synthesised by perfect blending of quinoline and 2-benzothiazoleacetonitrile unit. In a mixed aqueous solution, **HQCN** reacts with hydrazine (N<sub>2</sub>H<sub>4</sub>) to give a new product 2-(hydrazonomethyl)-8-methoxyquinoline along with the liberation of 2-benzothiazoleacetonitrile moiety. Contrariwise, the reaction of hypochlorite ion (OCl<sup>-</sup>) with the probe gives 8-methoxyquinoline-2-carbaldehyde. In both the cases, the chemodosimetric approaches of hydrazine and hypochlorite selectively take place at the olefinic carbon, but give two different products with two different outputs as observed from the fluorescence study exhibiting signal at 455 nm and 500 nm, respectively, for hydrazine and hypochlorite. The UV-vis spectroscopy study also depicts a distinct change in the spectrum of **HQCN** in presence of hydrazine and hypochlorite. The hydrazinolysis of **HQCN** exhibits a prominent chromogenic as well as ratiometric fluorescence change with a 165 nm left-shift in the fluorescence spectrum. Similarly, the probe in hand (**HQCN**) can selectively detect hypochlorite in a ratiometric manner with a shift of 120 nm as observed from the fluorescence emission spectra. **HQCN** can detect hydrazine and OCl<sup>-</sup> as low as  $2.25 \times 10^{-8}$  M and  $3.46 \times 10^{-8}$  M, respectively, as evaluated from the fluorescence experiments again. The excited state behaviour of the probe **HQCN** and the chemodosimetric products with hydrazine and hypochlorite are studied by the nanosecond time-resolved fluorescence technique. The computational study (DFT and TDDFT) with the probe and the hydrazine and hypochlorite product have also been performed. The observations made in the fluorescence imaging studies with human blood cells manifest that **HQCN** can be employed to monitor hydrazine and OCl<sup>-</sup> in human peripheral blood mononuclear cells (PBMCs). It is indeed a rare case that the single probe **HQCN** is found to be successfully able to detect hydrazine and hypochlorite in PBMCs, with two different outputs.

## 1. Introduction

Hydrazine is extensively used as the rocket propellant in space system<sup>1</sup>. It is an extremely important chemical reagent mainly used in pharmaceuticals, pesticides, emulsifiers, dyes and corrosion inhibitors in various chemical industries.<sup>2,3</sup> It is highly flammable and can be used for explosion.<sup>4</sup> On the other hand, hydrazine is regarded as a model industrial toxin, which adversely affects human and animal health by damaging the nervous system.<sup>5</sup> Hydrazine can readily be introduced in human

by oral, dermal or inhalation routes of exposure.<sup>6</sup> Extensive investigations with laboratory animals strongly indicates that hydrazine is carcinogenic which could cause the lungs, livers and kidneys cancerous. EPA (U.S. Environmental Protection Agency) has marked hydrazine as an impending human carcinogen, whereas World Health Organization (WHO) has suggested its threshold limit value (TLV) as 10 ppb.<sup>7,8</sup> Therefore, in real samples, the concentration of N<sub>2</sub>H<sub>4</sub> must be controlled as lower than 10 ppb.

On the contrary, reactive oxygen species (ROS) play crucial roles in many physiological processes in biological bodies.<sup>9,10</sup> Hypochlorous acid (HOCl) is known to be one of the most important biologically ROS-sub species. The endogenous production of hypochlorite is due to the peroxidation of chloride ions (mitochondrial electron transport chain) catalysed by the enzyme, namely, myeloperoxidase (MPO)<sup>11</sup>. However, abnormal production of ROS is extremely harmful owing to variations in MPO levels. The excess concentration of OCl<sup>-</sup> mainly involves unwanted oxidation of biomolecules.<sup>12</sup> Such oxidative stress can lead to a variety of diseases involving DNA mutations, aberrant electron transport, disruption of calcium

<sup>a</sup> Department of Chemistry, Jadavpur University, Kolkata -700032, India. Email: [tkmondal\\_ju@yahoo.com](mailto:tkmondal_ju@yahoo.com)

<sup>b</sup> Durham University, Department of Chemistry, Durham, DH1 3LE, UK, Email: [sangita.das@durham.ac.uk](mailto:sangita.das@durham.ac.uk); [sangitadas2327@gmail.com](mailto:sangitadas2327@gmail.com), [sangita.das@kist-europe.de](mailto:sangita.das@kist-europe.de)

<sup>c</sup> KIST Europe Forschungsgesellschaft mbH, Campus E71, 66123 Saarbrücken, Germany

<sup>d</sup> Center for Novel States of Complex Materials Research, Seoul National University, Seoul 08826, Republic of Korea.

<sup>e</sup> Department of Biochemistry, University of Calcutta, Kolkata-700019, India

† Footnotes relating to the title and/or authors should appear here.

Electronic Supplementary Information (ESI) available: [details of any supplementary information available should be included here]. See DOI: 10.1039/x0xx00000x

homeostasis, activation of apoptosis, cardiovascular diseases, neuron degeneration, arthritis and cancer.<sup>13</sup> Several studies have been reported so far by the researchers based on the adverse impact of both hydrazine and hypochlorite towards flora and fauna,<sup>14-33</sup> albeit there is a significant room for improvement.

Some relevant reports highlighting the probes detecting hydrazine and hypochlorite through different detection methods<sup>34, 35</sup> are mentioned in this regard. Yu *et al.* and co-workers fabricated an ICT based probe to detect hydrazine,<sup>36</sup> but with a limitation of sensitivity in basic pH. The detection of hydrazine was hampered under basic conditions. In another two reports by Duan *et al.* and Wu *et al.*, a distinct naphthalimide based ICT mediated sensor were discussed which exhibited a selective demasking of the acetate group by the chemodosimetric approach of hydrazine.<sup>37, 38</sup> Few more studies are also there on the hydrazine sensor based on the chromatographic techniques,<sup>39-41</sup> mass spectrometry coupled with chromatography,<sup>42</sup> Raman spectroscopy<sup>43</sup> and capillary electrophoresis<sup>44</sup> etc. But in most of the cases, these methods are time-consuming and require expensive instrumentation for implementation which have some serious limitation for real-time monitoring.

On the other hand, the HOCl sensitive fluorescent sensors follow different sensing mechanisms, for instance, the deoxygenation of fluorescent oximes,<sup>45-46</sup> chlorination of thioesters or amides,<sup>47-48</sup> oxidations of thioethers to selenoxides,<sup>49-50</sup> etc. However, none of the above-mentioned literatures have been able to identify simultaneously two important toxic analytes, namely hydrazine and hypochlorite in human PBMCs with fluorescence imaging at two different outputs.

Therefore, the interest is still there to develop powerful ratiometric fluorescent switches for the dynamic tracking and detection of N<sub>2</sub>H<sub>4</sub> and OCl<sup>-</sup> in living systems with high sensitivity and good selectivity. Most importantly, a single sensor which is able to detect hydrazine and hypochlorite in PBMCs based on two different mechanism with two different outputs is extremely rare.

Thus, in continuation of our previous work,<sup>51-55</sup> we have introduced a new switch (**HQCN**) which can detect the toxic N<sub>2</sub>H<sub>4</sub> and OCl<sup>-</sup> in presence of other guest analytes with two different outputs. The synthesis, photophysical characteristics and applications of this probe are manifested with highlighting several essential features in detail in the following 'Results and Discussion' section which consists of eleven subsections. In the 2.1. subsection, entitled 'Synthesis of the probe', the fabrication of the probe has been discussed. Here, the 2-benzothiazoleacetonitrile moiety has been used as a new recognition site for the detection of N<sub>2</sub>H<sub>4</sub> and OCl<sup>-</sup> with two distinct outputs. The photophysical properties of **HQCN** in the presence of different guest analytes have been thoroughly examined and analysed based on the UV-vis and Fluorescence study in the next two subsections, 2.2 and 2.3. Here, the mixed aqueous solution of HQCN (10 μM in CH<sub>3</sub>OH-H<sub>2</sub>O; 1/4, v/v) was prepared in the presence of HEPES buffer (10 mM) solution at pH = 7.2). The study to verify the specificity of the probe

towards hydrazine and hypochlorite in particular is indeed important and is emphasized in the next subsection 2.4. entitled 'Selectivity Study' which inevitably infers the probe as an excellent fluorescence tool for the sensing of N<sub>2</sub>H<sub>4</sub> and OCl<sup>-</sup> at two different wavelength outputs without any interference. The comprehensive description of the sensing mechanisms associated can be found in the subsection 2.5. The aptness of a probe is indeed crucial and therefore is accomplished by studying the effect of pH and the kinetics of the probe towards the target species as demonstrated in the subsections 2.6 and 2.7. These studies substantiate the **HQCN** is stable in the physiological system near the neutral pH for employing as a biomarker and successfully promote the probe as a smart candidate for the prompt monitoring of hydrazine and hypochlorite. The lifetime of **HQCN** and it's the adducts (**HQCN**-N<sub>2</sub>H<sub>4</sub> and **HQCN**-OCl) in the excited state is also measured using the nano second time-resolved fluorescence technique and is found to be in the order of nano second (subsection 2.8). As a support, the computational calculations (DFT and TDDFT) are performed which validate the practical observation of the probe with N<sub>2</sub>H<sub>4</sub> and OCl<sup>-</sup> as mentioned in the subsection 2.9.

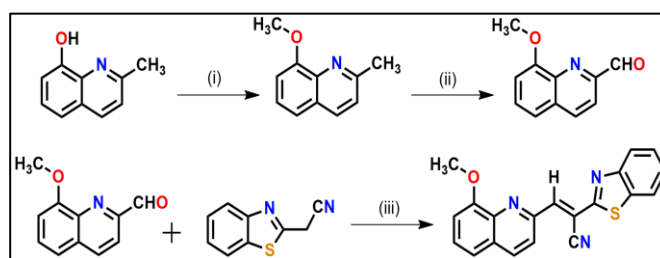
As far as the application of the probe is concerned, the bioimaging studies of **HQCN** are performed and is described in the subsection 2.10. The Cell viability study explains that this fluorescent probe does not hamper any cellular damages while the bioimaging of human PBMCs by **HQCN** reflects it as an excellent tool to distinguish N<sub>2</sub>H<sub>4</sub> and OCl<sup>-</sup> at two different wavelength outputs.

However, the detail synthetic procedure of the probe can be found in the 'Experimental' and the key findings are summarized in the 'Conclusion' section.

## 2. Results and discussion

### 2.1. Synthesis of the probe (HQCN)

The desired probe is synthesized as depicted in scheme 1. Firstly, 8-methoxyquinoline-2-carbaldehyde and 2-benzothiazoleacetonitrile are prepared according to the procedures reported elsewhere by our group<sup>56, 57</sup>.



**Scheme 1:** Synthesis of the receptor (**HQCN**). Reagents and conditions: (i) CH<sub>3</sub>I, K<sub>2</sub>CO<sub>3</sub> and acetone, refluxed for 5 h. (ii) SeO<sub>2</sub> and 1, 4-dioxane, refluxed for 4 h. (iii) piperidine and EtOH, refluxed for 2 h.

As per the Scheme 1, the condensation of 8-methoxyquinoline-2-carbaldehyde with 2-benzothiazoleacetonitrile in presence of a catalytic amount piperidine affords the probe (**HQCN**) as a yellow solid. The probe is characterised thereafter based on <sup>1</sup>H

NMR,  $^{13}\text{C}$  NMR and HRMS as shown in Figure S20–S22 in the supporting information. In addition, the structure of the probe in solid state is confirmed by measuring the single crystal X-ray diffraction of the sample. The ORTEP plot with atom numbering scheme is shown in Figure S1 in the supporting information. The crystallographic data have been deposited to the Cambridge Crystallographic Data Center: Deposition numbers CCDC 1858041. A summary of the crystallographic data is provided in Table S1 in the supporting information.

## 2.2. UV–vis study

The developed sensor **HQCN** is supposed to show a notable UV-vis change upon addition of hydrazine. In other words, the sensor has been fabricated in such a way that only hydrazine can play a chemodosimetric mechanism among the other elements and leads to the prominent change. However, the preliminary optical characteristics were investigated by monitoring the UV-vis absorption study by taking the probe, **HQCN** in a mixed aqueous methanol medium. It was observed that in absence of any guest analytes the probe exhibited an absorbance maximum at 370 nm. The experiment was duly repeated for several times and each time the strong absorbance peak appeared at 370 nm. This indicates that the probe in hand is highly stable under these physiological conditions. On the contrary, the addition of a trace amount of hydrazine causes a distinct change in the UV-vis profile. The absorption at 370 nm gradually decreased and a gradual increase in the absorption band at 272 nm was found at the same time (Figure 1a).

In order to understand the mechanism more clearly and to make the probe more suitable for environmental and biological applications, an optimized mixed aqueous solution was prepared. The detail constituent of the solution prepared was 10  $\mu\text{M}$  probe in a mixture of  $\text{CH}_3\text{OH}$  and  $\text{H}_2\text{O}$  with a volume ratio of 1:4 in the presence of 10 mM HEPES buffer solution at a pH of 7.2. Thereafter, the selectivity of the probe was verified in presence of several guest analytes such as hydroxylamine, ammonia, ethylenediamine, hydrazine, methylamine, n-butylamine, thiourea and triethylamine. It was worth noting that the probe acted promptly only after addition of hydrazine, whereas the other aforementioned amines remained almost mute to exhibit any significant change in the UV-vis spectroscopy (Figure 1b). After gradual addition of hydrazine from 0 to 5 equivalent, we found a characteristic change in the absorption spectra where the peak at 370 nm rapidly decreased and a new peak appeared at 272 nm with a well-defined isosbestic point at 292 nm (Figure 1). We consider that the change in the absorbance profile after addition of hydrazine may be attributed to the chemodosimetric approach of hydrazine to the olefinic carbon which rearranges to provide the reaction-based product, 2-(hydrazonomethyl)-8-methoxyquinoline. The absorbance at 272 nm has been plotted with the increasing concentration of hydrazine in this regard which clearly shows a good linear relationship in the range of 0–7.2  $\mu\text{M}$  with the  $R^2$  of 0.99 (Figure S6, supporting information).

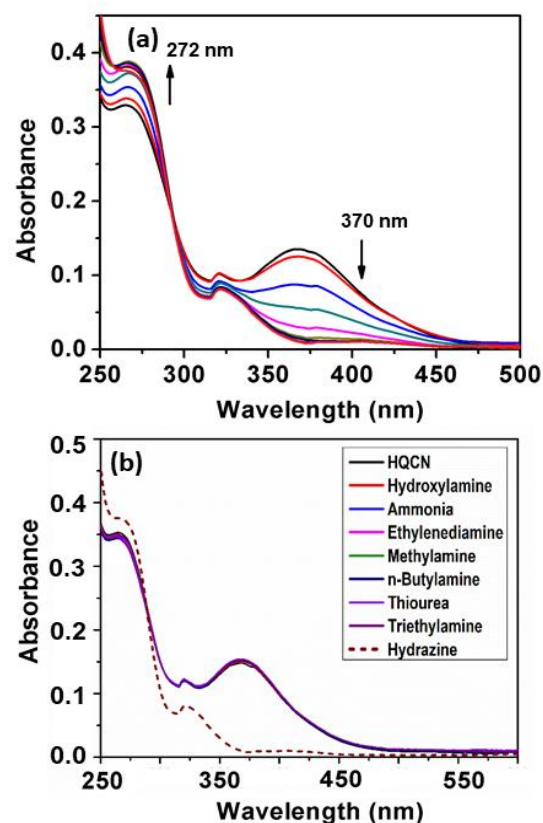


**Figure 1:** (a) UV-vis spectra of **HQCN** (10  $\mu\text{M}$  in  $\text{CH}_3\text{OH}$ - $\text{H}_2\text{O}$ ; 1/4, v/v in the presence of HEPES buffer (10 mM) solution at pH = 7.2) upon gradual addition of  $\text{N}_2\text{H}_4$  (0 to 5 equivalents). Ratiometric spectra of **HQCN** was observed after addition of  $\text{N}_2\text{H}_4$ . The absorption peak of **HQCN** at 370 nm gradually decreased and the peak at 272 nm gradually increased after addition of  $\text{N}_2\text{H}_4$  with an isosbestic point at 292 nm, (b) UV-vis spectra of **HQCN** (10  $\mu\text{M}$  in  $\text{CH}_3\text{OH}$ - $\text{H}_2\text{O}$ ; 1/4, v/v in the presence of HEPES buffer (10 mM) solution at pH = 7.2) upon addition of different guest analytes (Addition of different guest amines from 0 to 5 equivalents). Apart from hydrazine, no significant change was observed for other amines.

The absorption phenomena of **HQCN** towards different ROS were investigated further following the same process as hydrazine as described above. The constituents of the solution were also kept exactly same during this study. The solution of **HQCN** in the mixed aqueous media showed a strong absorbance at 370 nm. Interestingly, upon addition of  $\text{OCl}^-$  to the colourless solution of **HQCN**, the peak at 370 nm decreased evidently and a low-energy absorption band centred at 512 nm started appearing (Figure 2a). The isosbestic point was observed at 462 nm in this case. The change in the absorption behaviour here is attributed to the oxidation of the imine functionalized to the corresponding aldehyde (HQA) system. It was again striking to observe that the other guest analytes of interest, namely,  $\text{H}_2\text{O}_2$ ,  $\text{S}^{2-}$ ,  $\text{N}_3^-$ ,  $\text{NO}_2^-$ ,  $\text{NO}_3^-$ ,  $\text{I}^-$ ,  $\text{Cl}^-$ ,  $\text{F}^-$ ,  $\text{SO}_4^{2-}$ ,  $\text{ONOO}^-$ ,  $\text{O}^{2-}$  and t-BuOOH 10  $\mu\text{M}$ ,  $\text{H}_2\text{O}$  did not able to affect the UV-vis spectra of **HQCN** to a considerable extent (Figure 2b). The change in the absorbance of **HQCN** at 512 nm in the UV-vis spectrum was plotted with the added  $\text{OCl}^-$  concentration and a good linear relationship was observed here as well with a good  $R^2$  value of 0.99 (Figure S7, supporting information).

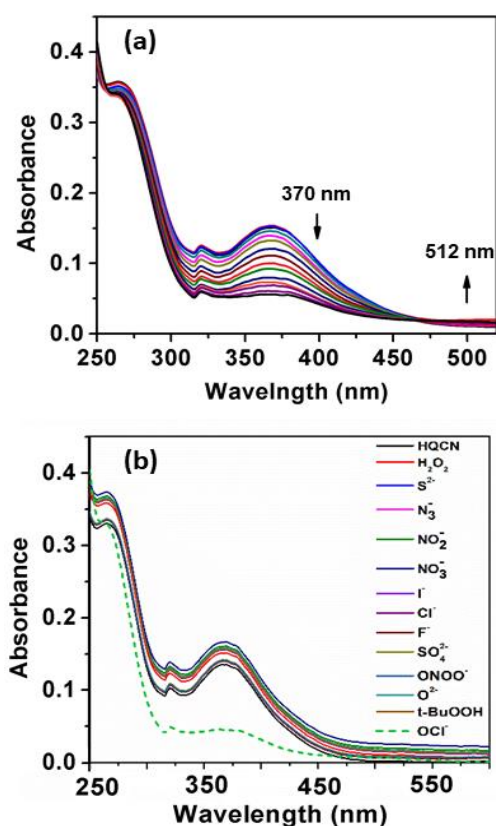


**Figure 2:** (a) UV-vis spectra of HQCN (10  $\mu\text{M}$  in  $\text{CH}_3\text{OH-H}_2\text{O}$ ; 1/4, v/v in the presence of HEPES buffer (10 mM) solution at pH = 7.2) upon gradual addition of  $\text{OCl}^-$  (0 to 5 equivalents). Ratiometric spectra of HQCN was observed after addition of  $\text{OCl}^-$ . The absorption peak of HQCN at 370 nm gradually decreased and the peak at 512 nm gradually increased after addition of  $\text{OCl}^-$  with an isosbestic point at 462 nm, (b) UV-vis spectra of HQCN (10  $\mu\text{M}$  in  $\text{CH}_3\text{OH-H}_2\text{O}$ ; 1/4, v/v in the presence of HEPES buffer (10 mM) solution at pH = 7.2) upon addition of different guest analytes (0 to 5 equivalents). Apart from  $\text{OCl}^-$ , no significant change was observed upon addition of other guest analytes.

### 2.3. Fluorescence study

In addition, we have monitored the spectral behaviour of HQCN based on the fluorescence study. In this study, the spectroscopic evaluation of the probe was carried out at room temperature in the mixed aqueous methanol solution similar to the UV-vis absorption measurement (10  $\mu\text{M}$  probe in  $\text{CH}_3\text{OH/H}_2\text{O}$ ; 1/4, v/v in presence of 10 mM HEPES buffer solution at pH, 7.2). Upon excitation at 370 nm, the probe in hand exhibited a strong emission peak with a maximum at 620 nm.

As per our expectation, no significant signal was appeared at 455 nm which evidences that the probe is stable in this mixed aqueous solution. But, based on the ICT (internal charge transfer) mechanism, significant changes in the fluorescence emission properties can occur in presence of hydrazine in the mixed aqueous solution of HQCN. Therefore, the fluorescence spectra have been recorded systematically upon the addition of hydrazine and other amines in the mixed aqueous solution of HQCN at room temperature. After interaction with hydrazine, the peak at 620 nm gradually decreased, whereas a concomitant new peak was observed at 455 nm with an increased intensity through a well-defined isoemissive point at 520 nm (Figure 3a). In order to understand the

chemodosimetric mechanism more clearly, we studied the reaction of hydrazine with the probe in hand by measuring the mass spectra.

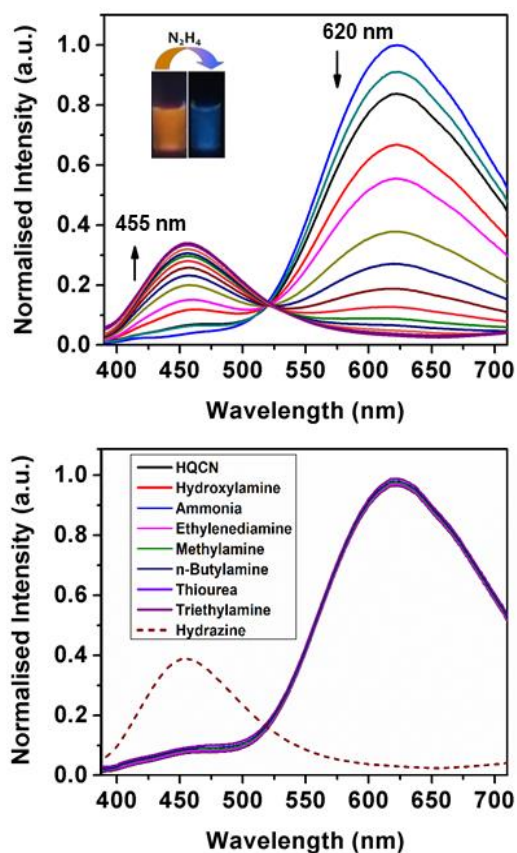


**Figure 3:** (a) Fluorescence emission spectra of HQCN (10  $\mu\text{M}$  in  $\text{CH}_3\text{OH-H}_2\text{O}$ ; 1/4, v/v in the presence of HEPES buffer (10 mM) solution at pH = 7.2) upon gradual addition of  $\text{N}_2\text{H}_4$  (0 to 5 equivalents) where the  $\lambda$  excitation was 370 nm. Ratiometric spectra of HQCN was observed after addition of  $\text{N}_2\text{H}_4$ . The emission peak of HQCN at 620 nm gradually decreased and the peak at 455 nm gradually increased after addition of hydrazine with an isoemissive point at 520 nm. Inset shows the visible emission of HQCN in absence and presence of 2 equivalents of hydrazine upon irradiation under UV light, (b) Fluorescence emission spectra of HQCN (10  $\mu\text{M}$  in  $\text{CH}_3\text{OH-H}_2\text{O}$ ; 1/4, v/v in the presence of HEPES buffer (10 mM) solution at pH = 7.2) after addition of different guest analytes (0 to 5 equivalents). Apart from hydrazine, no significant change was observed for other guest amines.

A prominent peak observed in the MS spectrum at  $m/z$ , 202.1212 may represent the characteristics of the in-situ product i.e., the HQCN- $\text{N}_2\text{H}_4$ -adduct (Fig S23, supporting information), which supports the proposed sensing mechanism. After addition of hydrazine, the increase in the emission intensity at 455 nm was noticed which was associated with the hydrazinolysis at the olefinic carbon of HQCN indeed. This further got conjugated at nitrile portion and eventually liberated the recognition sight i.e., 2-benzothiazoleacetonitrile. This mechanism may play the ICT enhancement by forming the in-situ adduct HQCN- $\text{N}_2\text{H}_4$  as depicted in Scheme 2.

The fluorogenic response of HQCN has been studied as well applying several other important amines. Analogous to the absorption phenomena, almost all the guest amines including hydroxylamine, the well-known interfering compound with hydrazine were found to be sufficiently non-responsive towards HQCN (Figure 3b). Only hydrazine was able to make a distinct ratiometric change along with a significant left-shift of around



165 nm in the fluorescence spectra. This interesting feature was further confirmed when no significant changes in the emission spectrum of the receptor was observed upon performing the experiment in presence of the excess amount of the guest amines. Therefore, the probe in this study is quite exclusive in detecting hydrazine among the other important amines. In this context, we have provided a table where the performance of our probe in hand is compared with other reported fluorescence sensors (Comparison Table S4 in the supporting information). However, the ratio of the emission intensity of HQCN at 455 and 620 nm ( $I_{455}/I_{620}$ ) has been plotted with the added concentration of hydrazine. A good linear relationship was found here as well with the  $R^2$  of 0.99 (Figure S4, supporting information). From the plot based on the emission spectra, the limit of detection (LOD) of hydrazine was evaluated thereafter following the equation,  $DL = K \times (Sb1/S)$ , where 'K' is considered as 3 and 'Sb1' and 'S' define the standard deviation of the blank solution and the slope of the calibration curve, respectively<sup>58,59</sup>. The calculated detection limit was  $2.25 \times 10^{-8}$  M (Figure S4, supporting information) which inevitably ensures that the HQCN has a very good efficiency to detect the hydrazine. In addition, the quantum yields of HQCN and HQCN- $N_2H_4$  adducts were calculated using the rhodamine-B ( $\phi = 0.66$  in ethanol) as reference and those were 0.39 and 0.24 respectively.

During the observation of the fluorescence behavior of the compound HQCN in presence of  $OCl^-$ , the constituent of the solution has been kept same as the previous experiments (10  $\mu$ M probe in  $CH_3OH/H_2O$ ; 1/4, v/v in presence of 10 mM HEPES buffer solution at pH, 7.2). Here, the main emission band of HQCN at 620 nm was got completely quenched upon addition of  $OCl^-$ , whereas a new peak at 500 nm was found to arrive as observed in Figure 4a. This was a convincing evidence for the probe as  $OCl^-$  sensor when we observed that the fluorescence intensity of HQCN remained almost unperturbed in presence of the other guest analytes, namely,  $H_2O_2$ ,  $S^{2-}$ ,  $N_3^-$ ,  $NO_2^-$ ,  $NO_3^-$ ,  $I^-$ ,  $Cl^-$ ,  $F^-$ ,  $SO_4^{2-}$ ,  $OONO^-$ ,  $O^{2-}$  and t-BuOOH (Figure 4b). The trend of the emission intensity was found to get decreased with increasing the concentration of  $OCl^-$ . We are assigning this phenomenon as the conversion of the imine group to the corresponding formyl group (aldehyde). A large shift of 120 nm was observed in this ratiometric spectrum. This large emission shift ( $\Delta F = 120$  nm) has been attributed to the accurate measurement of the intensities between the two emission peaks with a high ratiometric value. This chemodosimetric reaction of  $OCl^-$  to the imine functionality of HQCN eventually produced the oxidised product i.e., the HQCN- $OCl^-$  adduct (8-methoxyquinoline-2-carbaldehyde). The formation of this in-situ adduct was further confirmed by recording the mass spectra and  $^1H$  NMR titration of HQCN after the addition of  $OCl^-$  (Figure S24 and S25c, respectively, supporting information). The calculated quantum yield of the HQCN- $OCl^-$  adduct was 0.45. The plot of the fluorescence intensity ratio at 500 and 620 nm ( $I_{500}/I_{620}$ ) versus the added  $OCl^-$  concentration exhibited a good linear relationship with the  $R^2$  value (Figure S5, supporting information). The ratiometric probe exhibited a detection limit of  $3.46 \times 10^{-8}$  M for  $OCl^-$  (Figure S5, supporting information). It

was calculated from the fluorescence experimental data similarly as calculated for the hydrazine. Other potentially competing guest analytes did not hamper the recognition of hypochlorite anion. Herein, HQCN is acting as a fast-responding and highly sensitive sensor for the detection of  $OCl^-$ .

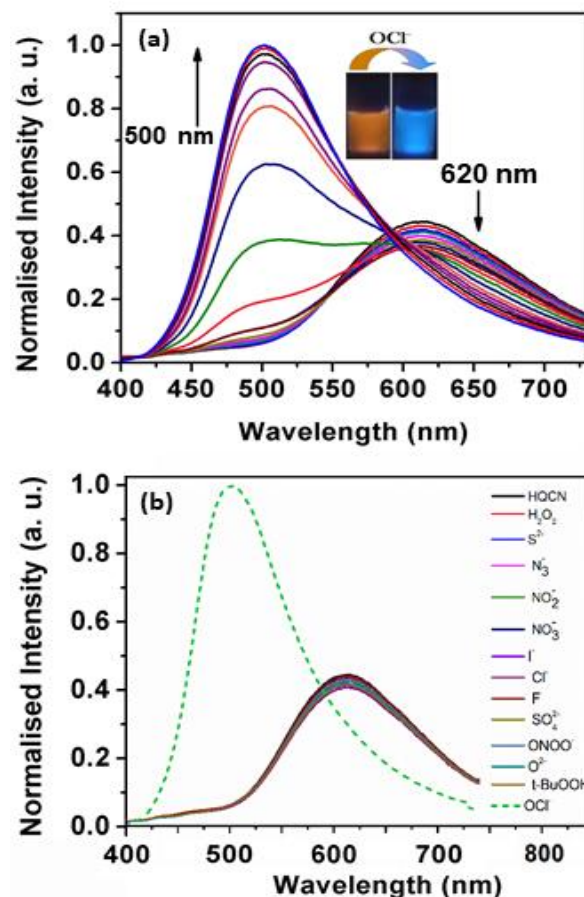


**Figure 4:** (a) Fluorescence emission of HQCN (10  $\mu$ M in  $CH_3OH-H_2O$ ; 1/4, v/v in the presence of HEPES buffer (10 mM) solution at pH = 7.2) upon gradual addition of  $OCl^-$  (0 to 5 equivalents). Ratiometric spectra of HQCN was observed after addition of  $OCl^-$  where the  $\lambda$  excitation was 370 nm. The fluorescence emission peak at 620 nm gradually decreased and the peak at 500 nm gradually increased after addition of  $OCl^-$ . Inset shows the visible emission of HQCN in absence and presence of 2 equivalents of HOCl upon irradiation under UV light. (b) Fluorescence emission spectra of HQCN (10  $\mu$ M in  $CH_3OH-H_2O$ ; 1/4, v/v in the presence of HEPES buffer (10 mM) solution at pH = 7.2) upon addition of different guest analytes (0 to 5 equivalents). Apart from  $OCl^-$ , no significant change was observed for other guest analytes.

#### 2.4. Selectivity study

Selectivity and sensitivity are the two very important constraints for assessing the performance of any chemodosimeters and chemosensors. In order to measure the selectivity, the experiment was performed with the probe in hand (HQCN) in presence of the target species and the series of other guest analytes as mentioned above. Firstly, the specificity of the probe towards hydrazine was verified in addition of other important amines. To execute this experiment, the fluorescence intensity of the solutions of the HQCN and 2 equivalents of  $N_2H_4$  at 455 nm were sequentially measured after addition of different guest amines in much excess concentration of  $\sim 3$

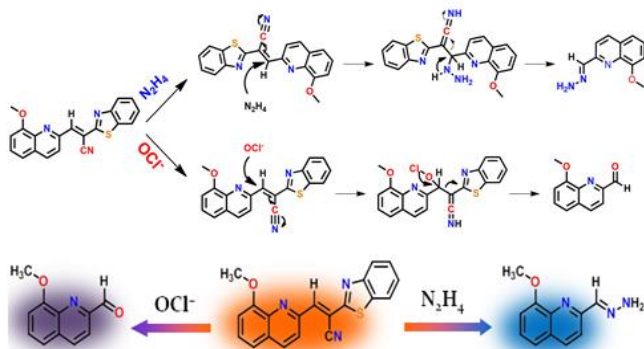
equivalents (Figure S2, supporting information). After observing the result, it was clear that the detection of hydrazine by **HQCN** was not at all hampered even in the presence of other interfering guest amines in excess amount.

Likewise, the sensitivity of **HQCN** towards  $\text{OCl}^-$  was studied as well by measuring the fluorescence output at 500 nm. The emission intensity of **HQCN** at 500 nm was measured in the same way after treatment of  $\text{OCl}^-$  (2 equivalents) in presence of the other guest analytes (3.0 equivalents). In this case also it was quite evident that the recognition of  $\text{OCl}^-$  in the presence of other relevant analytes was not either hampered (Figure S3, supporting information).

Therefore, we can firmly conclude that the probe in hand **HQCN** can be employed as a sensitive fluorescence tool for the detection of  $\text{N}_2\text{H}_4$  and  $\text{OCl}^-$  at two different outputs with no significant interference.

## 2.5. Sensing mechanism of the probe

To get insight into the proposed sensing process, we studied the reaction of **HQCN** with  $\text{N}_2\text{H}_4$  and  $\text{OCl}^-$ , respectively, based on the mass spectrometry. When **HQCN** (20  $\mu\text{M}$ ) was treated with  $\text{N}_2\text{H}_4$  (80  $\mu\text{M}$ ), a significant peak (Figure S23, supporting information) was observed at  $m/z$  202.1212 which is consistent with the value estimated with the reaction-based product, **HQCN**- $\text{N}_2\text{H}_4$ -adduct (expected  $[\text{M}+\text{H}]^+$  at 202.0980, Figure S23, supporting information). The reaction mechanism is demonstrated as Scheme 2.



**Scheme 2:** Plausible mechanism for the recognition of  $\text{N}_2\text{H}_4$  and  $\text{OCl}^-$  by **HQCN**. The probe in hand “two-way” detects hydrazine and hypochlorite via two different “dye-release” mechanisms.

We have also analysed the reaction product **HQCN**- $\text{OCl}^-$  (**HQA**) adduct (Figure S24, supporting information). The chemodosimetric reaction-based product finally gave the corresponding aldehyde within a few seconds. This product was isolated for spectrochemical studies. The peak at 242.2538  $m/z$  is consistent with the expected formylation product (expected  $[\text{M}+\text{H}_2\text{O}+\text{Cl}^-+2\text{H}^+]^+$  at 242.0589). The plausible chemodosimetric mechanism between **HQCN** and  $\text{OCl}^-$  is depicted as Scheme 2. **HQCN** was first oxidatively attacked by  $\text{OCl}^-$  to the imino group which further rearranged to form the formyl adduct (**HQA**).

## 2.6. Effect of pH

The effect of pH on the fluorescence response of **HQCN** towards  $\text{N}_2\text{H}_4$  and  $\text{OCl}^-$ , respectively, was also explored. The probe itself showed an insignificant change in the fluorescence intensity throughout the wide range of pH from 2.0 to 12. This strongly recommends that the **HQCN** is stable in the wide pH range and can be successfully applied in the biological samples. Thereafter, we recorded the changes in the fluorescence of **HQCN** after treatment with hydrazine. We found that at acidic pH the **HQCN**- $\text{N}_2\text{H}_4$  system exhibited no significant change in the fluorescence spectrum, more specifically the emission intensity at 455 nm (Figure S8a, supporting information). On the contrary, at basic pH, above 8.3 in particular, a huge influence was observed towards the detection of hydrazine through a significant change in the emission intensity at 620 nm (Figure S8b, supporting information). This experiments again supports the reliability of **HQCN** as an efficient fluorescence tool for the detection of hydrazine in biological pH.

Also, we have examined the pH sensitivity of the **HQCN**- $\text{OCl}^-$  adduct (**HQA**). The **HQA** was quite sensitive towards the acidic pH (Figure S9, supporting information) as an enhancement in the emission intensity at 620 nm was observed, especially above pH 6. Therefore, based on all these findings, we can unambiguously proclaim the probe as a potential biomarker in the bio samples.

## 2.7. Response rate

The reaction kinetics is a very important factor in terms of justifying the performance of any chemodosimeter. In the present study, we have calculated the rate constants of the two chemodosimetric reactions. In both cases, the fluorescence emission intensity of **HQCN** increased successively with increasing the duration of the reaction with hydrazine and hypochlorite. Most importantly, the interaction of **HQCN** towards hydrazine and hypochlorite was found to be completed within a few seconds. The rate constant of the reactions between **HQCN** and hydrazine and **HQCN** and hypochlorite has been calculated in this regard. For that, firstly, the fluorescence spectra of **HQCN** were recorded after addition of two equivalents of hydrazine. The fluorescence intensity at 455 nm was plotted with the reaction duration which offered a linearity up to around 50 seconds only, and afterwards, no such increment was noticed with the progression in the reaction time (Figure S10, supporting information). Following the first order rate equation, the rate constant ( $k$ ) i.e., the slope of the plot  $\times 2.303$  was calculated which was  $5.72 \times 10^{-2} \text{ sec}^{-1}$ .

The kinetic study was performed in the same way after interaction of **HQCN** with  $\text{OCl}^-$ . A noteworthy increment in the emission intensity at 500 nm was observed and it reached the maxima at around 55 seconds (Figure S11, supporting information). Based on the plot of the fluorescence intensity at 500 nm versus the duration of the reaction, the pseudo first order rate constant ( $k$ ) was calculated. The calculated rate constant was found to be  $8.33 \times 10^{-2} \text{ sec}^{-1}$  for this reaction.

The considerably higher rate constants of the reactions demonstrate that our synthesized probe, **HQCN** can also be

effectively used as a real-time monitoring kit for hydrazine and hypochlorite at two different outputs.

## 2.8. Lifetime

We have also examined the excited state behaviour of the probe **HQCN** and its reaction with hydrazine and hypochlorite based on the nano second time-resolved fluorescence technique as exhibited in Figure 5. In this study, the radiative rate constants were calculated according to the equation  $60 \tau^{-1} = k_r + k_{nr}$ , where  $k_r$  which can be related to the emission quantum yield and lifetime as  $\Phi_f / \tau$  defines the radiative rate constant, whereas  $k_{nr}$  defines the non-radiative rate constant of **HQCN** and the adducts, namely **HQCN-N<sub>2</sub>H<sub>4</sub>** and **HQCN-OCl<sup>-</sup>** (**HQA**). The calculated rate constants are mentioned in Table S2 in the supporting information. The calculated  $\tau$  was found to be 0.7 ns ( $\chi^2 = 1.21$ ) for **HQCN**, 6.32 ns ( $\chi^2 = 1.15$ ) for **HQCN+N<sub>2</sub>H<sub>4</sub>** and 5.75 ns ( $\chi^2 = 1.09$ ) for **HQCN+ OCl<sup>-</sup>**.

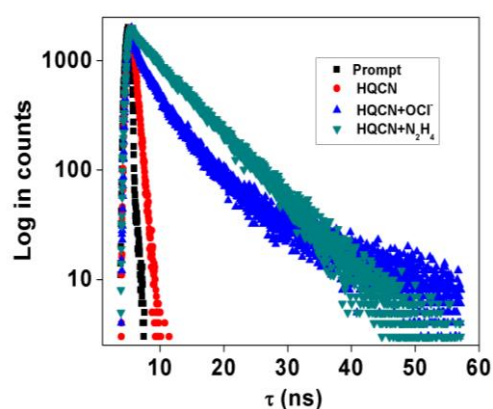


**Figure 5:** Time-resolved fluorescence decay of **HQCN** (red), **HQCN+OCl<sup>-</sup>** (blue), **HQCN+N<sub>2</sub>H<sub>4</sub>** (green) and prompt (black) ( $\lambda$  excitation = 370 nm). The calculated  $\tau$  was 0.7 ns ( $\chi^2 = 1.21$ ) for **HQCN**, 6.32 ns ( $\chi^2 = 1.15$ ) for **HQCN+N<sub>2</sub>H<sub>4</sub>** and 5.75 ns ( $\chi^2 = 1.09$ ) for **HQCN+ OCl<sup>-</sup>**.

## 2.9. Computational study

In this section, we have studied the relationship between the structural changes of **HQCN** and its complexes (with hydrazine and hypochlorite) and their optical responses. This theoretical calculation was evaluated by the Density Functional Theory (DFT) and the Time Dependent Density Functional Theory (TDDFT) with the B3LYP/6-31+G(d) method in Gaussian 09W, Revision D.01 program and visualized using Gauss view program.<sup>61-62</sup> The optimized geometry and the highest occupied molecular orbital (HOMO) and lowest unoccupied molecular orbital (LUMO) of **HQCN** are depicted in Figure S12, supporting information. For TDDFT calculation, solvent correction was incorporated by the CPCM model and methanol was chosen as the solvent. The calculated absorption spectra show peaks at 461.47 nm ( $f = 0.4150$ ), 392.12 nm ( $f = 0.6966$ ) and 373.11 nm ( $f = 0.0873$ ) for **HQCN**, which are due to HOMO to LUMO, HOMO-1 to LUMO, HOMO-2 to LUMO transitions, respectively (supporting information, Table S3). However, for reaction product (**HQCN-N<sub>2</sub>H<sub>4</sub>**), HOMO to LUMO+1 transition is appeared at 277.93 nm ( $f = 0.9427$ ), in case of the other reaction-based product a strong transition appeared at 253.42 nm ( $f = 0.5423$ )

corresponds to HOMO-2 to LUMO transition (Figure S13, S14, S15, supporting information).

## 2.10. Bioimaging and MTT assay

**HQCN** is an excellent intracellular switch to detect hydrazine for its permeability as well as stability. The figure 6 (a) describes the bioimaging of human PBMCs by **HQCN** when there is no added **N<sub>2</sub>H<sub>4</sub>** from outside. In figure 6 (b) very little or no blue fluorescence has been observed here. However, addition of **N<sub>2</sub>H<sub>4</sub>** significantly enhances the blue fluorescence (Figure 6 e) making it an excellent probe for bioimaging of **N<sub>2</sub>H<sub>4</sub>**. In Figure S16, supporting information, we can see that at the red channel **HQCN** has shown a prominent intensity at the red channel ( $2759.3 \pm 127.1$ ) without hydrazine. The hydrazine untreated cells show almost insignificant fluorescence intensities at blue channel ( $677.6 \pm 27.5$ ). However, after addition of hydrazine a significant increase ( $P < 0.05$ ) in blue fluorescence intensities was observed ( $3095 \pm 125.7$ ). Consequently, in this situation the red fluorescence got expressively ( $P < 0.05$ ) reduced ( $739 \pm 40.8$ ). The P values were evaluated by using the one-way ANOVA followed by multiple comparisons for differences between groups (Figure S16, supporting information).

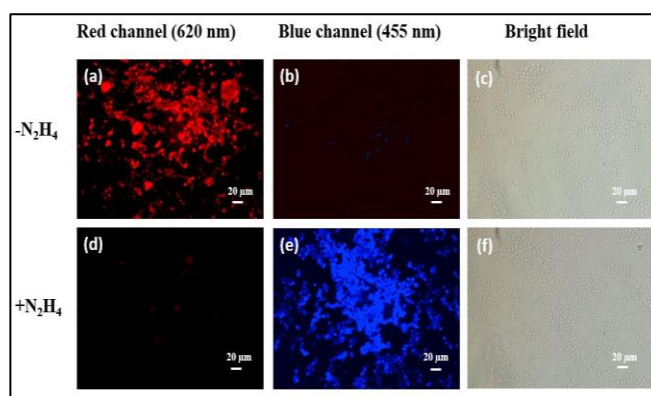


**Figure 6:** Fluorescence images (40X) of human peripheral blood mononuclear cells (PBMCs) treated with 10  $\mu$ M **HQCN** (a and b) and then the same was treated with 20  $\mu$ M hydrazine solution (d and e), respectively. Images were taken in red channel (620 nm) and blue channel (455 nm), ( $\lambda$  excitation = 370 nm). Larger cells are macrophages in PBMC populations, c and f are the corresponding bright-field images. The hydrazine untreated cells showed almost insignificant fluorescence intensities at blue channel, but showed a prominent color in the red channel, (a) However, after addition of hydrazine a significant increase in the blue fluorescence intensities was observed (e).

Cell viability was represented in Figure S17, supporting information, where up to 50  $\mu$ M concentrations of **HQCN** shows around 63.26% and 66.83 % of viable cells with and without the presence of **N<sub>2</sub>H<sub>4</sub>** respectively, predicting it is a safe probe to use in a biological system. We have used 20  $\mu$ mol/l **HQCN** solutions for imaging which shows fairly high number of viable cells (78.09 %) in presence of **N<sub>2</sub>H<sub>4</sub>** concluding its nontoxic nature.

**HQCN** is an excellent probe for imaging of biological samples for its permeability and stability. This fluorescent probe does not cause any cellular damages. Figure 7, depicts the bioimaging of human PBMCs by **HQCN** in absence and presence of **OCl<sup>-</sup>**.

Therefore, synthesis of non-toxic fluorescence probe to detect HOCl is of extreme importance. In this present study, in absence of **OCl<sup>-</sup>** the shifting from red fluorescence to green fluorescence



is very less significant but after addition of  $\text{OCl}^-$  a prominent increase in green fluorescence has been observed. The mean fluorescence intensities were measured in ImageJ (Figure S18, supporting information). The P values were calculated by using one-way ANOVA followed by multiple comparison for differences between the groups. The MTT assay (Cell viability) was represented in Figure S19, supporting information, where increasing the concentrations of **HQCN** up to 50  $\mu\text{M}$  shows the viable cells with and without  $\text{OCl}^-$  were 53.73% and 56.18 % respectively

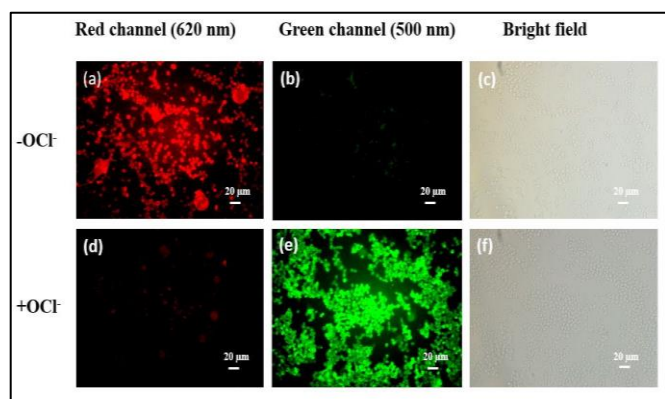


**Figure 7:** Human PBMCs (40X) treated with 10  $\mu\text{mol/l}$  **HQCN** under fluorescence emissions of 620 nm (a and d) and 500 nm (b and e), respectively. Images were captured before and after 50 minutes of incubation at dark. The cells showed almost insignificant fluorescence intensities at green channel in absence of  $\text{OCl}^-$  but showed a prominent color in the red channel (b and a respectively). However, in presence of  $\text{OCl}^-$  a significant increase in the green fluorescence intensities was observed (e).

### 2.11. Application as Test-Kit

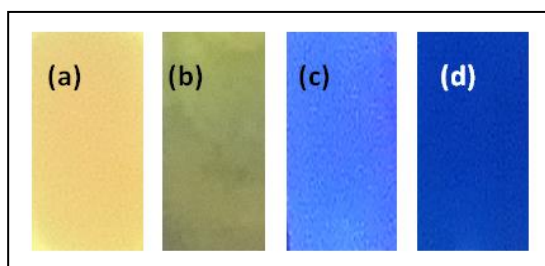


**Figure 8:** Photographs of TLC plates, soaked in the solution of (a) **HQCN** and (b, c, d) after bubbling with hydrazine contaminated air. Pictures taken after (b) 10 sec; (c) 60 sec (d) 5 min.

Inspired by the superior sensitivity of **HQCN** towards hydrazine and hypochlorite, we have further explored the probe for the detection of these species even in trace amount. These experiments were mainly performed just to provide a qualitative idea whether **HQCN** can be explored as a portable kit for sensing hydrazine and hypochlorite. To execute these experiments, a TLC plate was immersed in the 0.10 mM **HQCN** solution in  $\text{CH}_3\text{OH}$  and was dried in air.

After bubbling a large amount of contaminated air mixed with hydrazine, the **HQCN** loaded TLC plate displayed prominent changes of colour. We have recorded the fluorescence change with time by capturing the photographs of the particular TLC

plate at different time intervals. After the exposure of the hydrazine vapour, the color of the TLC plate changed within 10 seconds where it was monitored up to 5 minutes.

However, the distinct change of the color of the plate can be observed in Figure 8 b-d. This promising result again recommends that the probe in hand **HQCN** can be employed as a highly sensitive candidate for the instant detection of the hydrazine and corroborates our previous inferences.

The similar experiment was conducted for the detection of  $\text{OCl}^-$  as depicted in Figure 9. The clearly distinguishable color change of the TLC plate also suggests that the probe offers a good portable assay kit for the hypochlorite sensor as well.

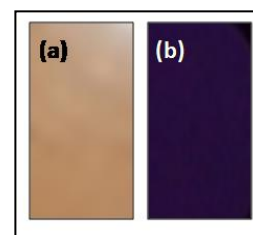


**Figure 9:** Photographs of TLC plates, soaked in the solution of (a) **HQCN** and (b) after treating with  $\text{OCl}^-$  (Pictures taken after 5 min).

## 3. Experimental

### Synthesis of the probe (**HQCN**)

8-methoxyquinoline-2-carbaldehyde (0.5 g, 2.67 mmol) and benzothiazole-2-yl-acetonitrile (0.47 g, 2.70 mmol) were added together in ethanol (10 mL) solution and stirred at room temperature for 10 minutes. Piperidine (50  $\mu\text{L}$ ) and a catalytic amount of acetic acid were added subsequently to the reaction mixture and reflux for 2 h under  $\text{N}_2$ -atm. Yellow colored precipitate was formed after cooling the reaction mixture to the room temperature which was collected through filtration. The crude residue was purified through column chromatography using EtOAc/Petroleum ether (1/4, v/v) as eluent. Yield = 72%.

$^1\text{H NMR}$  (300 MHz,  $\text{CDCl}_3$ ):  $\delta$  4.16 (s, 3H), 7.13 (d,  $J = 6.9$  Hz, 1H), 7.45 (t,  $J = 6.9$  Hz, 2H), 7.55 (t,  $J = 7.6$  Hz, 2H), 7.93 (d,  $J = 7.3$  Hz, 1H), 8.13 (d,  $J = 8.0$  Hz, 1H), 8.34 (dd,  $J_1 = 8.6$  Hz,  $J_2 = 8.6$  Hz, 2H), 8.51 (s, 1H).

$^{13}\text{C NMR}$  (75 MHz,  $\text{CDCl}_3$ ):  $\delta$  56.56, 108.63, 110.10, 115.83, 119.46, 121.73, 123.47, 126.45, 126.99, 129.07, 129.50, 135.23, 137.11, 140.44, 146.76, 149.77, 153.65, 155.90, 162.55.

**HRMS (ESI, positive):** calcd. for  $\text{C}_{20}\text{H}_{13}\text{N}_3\text{OS}$  [ $\text{M} + \text{H}$ ] $^+$  (m/z): 344.0858; found: 344.1226.

## 4. Conclusions

In this paper, a new ratiometric fluorescent switch **HQCN** has been introduced by the perfect combination of quinoline and 2-benzothiazoleacetonitrile unit. The probe was highly selective and sensitive in detecting both the hydrazine and hypochlorite in a mixed aqueous solution following two different chemodosimetric mechanisms and consequently with two



different emission outputs. The chemodosimetric hydrazinolysis of **HQCN** exhibited a ratiometric fluorescence change with a large left-shift of 165 nm and also can successfully detect hypochlorite in a ratiometric manner exhibiting a left-shift of 120 nm in the fluorescence emission spectra which unambiguously supports the diverse practical applications of the probe. Moreover, the quantitative detection of hydrazine and hypochlorite was found to be  $2.25 \times 10^{-8}$  M and  $3.46 \times 10^{-8}$  M, respectively. These low LOD (limit of detection) values reflect the high performance of the probe. Some reports can be found in this regard which claim to act as either hydrazine or hypochlorite sensor, although separately, while in most of the cases, the probes are not promising to detect simultaneously both hydrazine and  $\text{OCl}^-$  as mentioned in Table S4 in the supporting information. Therefore, this is indeed exceptional that a probe can selectively detect the toxic hydrazine as well as hypochlorite based on two different mechanism. Further, our probe in hand can be used as a real-time monitoring kit for the instant qualitative detection of  $\text{N}_2\text{H}_4$  and  $\text{OCl}^-$  in samples in a facile way, namely, by the dip-stick method which is quite commendable when we consider the performance of the other probes reported so far for the on-site as well as real-time visual monitoring of the hydrazine and  $\text{OCl}^-$ . Albeit, several important reports are available on the sensing of the hydrazine and  $\text{OCl}^-$ , but ample scopes are there for developing their potential. New probes with good water solubility, low cytotoxicity, excellent cell permeability from other molecular or ionic entities and compatibility for the live cell imaging are still in demand. The biological utility of the probe has also been established here based on the bioimaging studies which confirms the **HQCN** as a unique tool to distinguish hydrazine and hypochlorite anion for the first time in human PBMCs with two different outputs. A single sensor providing significant ratiometric changes in the physiological pH condition during the sensing of both the hydrazine and hypochlorite in an environmental aqueous system is also quite rare. Therefore, our study could pave the way for developing new probes with dual sensing ability.

## 5. Conflicts of interest

"There are no conflicts to declare".

## 6. Acknowledgements

Dr. S. Das thanks Science and Engineering Research Board (SERB), Govt. of India, for National Post-Doctoral Fellowship (NAPDF), File no. PDF/2016/001907 and Newton International Fellowships Royal Society (UK) for fellowship (ref: NIF\R1\182209). Prof. T. K. Mondal thanks to CSIR, New Delhi, India for financial support (No. 01(2992)/19/EMR-II). S. Das Acknowledges Dr. Krishnendu Aich, Department of Chemistry, Jadavpur University for helping in the excited state behaviour study of the compound.

## 7. Notes and references

- S. D. Zelnick, D. R. Mattie and P. C. Stepaniak, *Aviat., Occupational Exposure to Hydrazines: Treatment of Acute Central Nervous System Toxicity, Space Environ. Med.*, 2003, **74**, 1285–1291.
- S. S. Narayanan and F. Scholz, *A comparative study of the electrocatalytic activities of some metal hexacyanoferrates for the oxidation of hydrazine, Electroanalysis*, 1999, **11**, 465–469 ([https://doi.org/10.1002/\(SICI\)1521-4109\(199906\)11:7<465::AID-ELAN465>3.0.CO;2-%23](https://doi.org/10.1002/(SICI)1521-4109(199906)11:7<465::AID-ELAN465>3.0.CO;2-%23))
- K. Yamada, K. Yasuda, N. Fujiwara, Z. Siroma, H. Tanaka, Y. Miyazaki and T. Kobayashi, *Potential application of anion-exchange membrane for hydrazine fuel cell electrolyte, Electrochem. Commun.*, 2003, **5**, 892–896 (DOI: 10.1016/j.elecom.2003.08.015).
- U. Ragnarsson, *Synthetic methodology for alkyl substituted hydrazines, Chem. Soc. Rev.*, 2001, **30**, 205–213 (doi.org/10.1039/B010091A).
- International Agency for Research on Cancer, Re-evaluation of some organic chemicals, hydrazine, and hydrogen peroxide. IARC Monographs on the Evaluation of Carcinogenic Risk of Chemicals to Humans, IARC, Lyon, 1999, vol. 71, pp. 991–1013, <http://monographs.iarc.fr/ENG/Monographs/vol71/mono71-43.pdf>.
- Z. An, Z. Li, Y. He, B. Shi, L. Wei and M. Yu, *Ratiometric luminescence detection of hydrazine with a carbon dots-hemicyanine nanohybrid system, RSC Adv.*, 2017, **7**, 10875–10880 (doi.org/10.1039/C6RA27844B).
- U.S. Environmental Protection Agency, Integrated Risk Information System (IRIS) on Hydrazine/Hydrazine Sulfate, National Center for Environmental Assessment, Office of Research and Development, Washington, D.C, 1999.
- A. Umar, M. M. Rahman, S. H. Kim and Y.-B. Hahn, *Zinc oxide nanonail based chemical sensor for hydrazine detection, Chem. Commun.*, 2008, 166–168 (doi.org/10.1039/B711215G).
- X. Chen, X. Tian, I. Shin and J. Yoon, *Fluorescent and luminescent probes for detection of reactive oxygen and nitrogen species, Chem. Soc. Rev.*, 2011, **40**, 4783–4804, *Chem. Soc. Rev.*, 2011, **40**, 4783–4804 (doi.org/10.1039/C1CS15037E).
- A. Gomes, E. Fernandes and J. L. F. C. Lima, *Fluorescence probes used for detection of reactive oxygen species, J. Biochem. Biophys. Methods*, 2005, **65**, 45–80 (doi: 10.1016/j.jbbm.2005.10.003).
- N. Zhao, Y. H. Wu, R. M. Wang, L. X. Shi and Z. N. Chen, *An iridium(III) complex of oximated 2,2'-bipyridine as a sensitive phosphorescent sensor for hypochlorite, Analyst*, 2011, **136**, 2277–2282 (doi.org/10.1039/C1AN15030H).
- M. Whiteman, D. C. Hooper, G. S. Scott, H. Koprowski and B. Halliwell, *Inhibition of hypochlorous acid-induced cellular toxicity by nitrite, Proc. Natl. Acad. Sci. U. S. A.*, 2002, **99**, 12061–12066 (doi: 10.1073/pnas.152462399).
- W. Y. Lin and L. L. Long, B. B. Chen, W. Tan, *A Ratiometric Fluorescent Probe for Hypochlorite Based on a Deoxygenation Reaction, Chem.-Eur. J.*, 2009, **15**, 2305–2309 (DOI: 10.1002/chem.200802054).
- G.-F. Wu, M.-X. Li, Y. Zhang, W.-G. Ji, Q.-B. Wang and Q.-X. Tong, *Materials and Electronics Engineering*, 2014, **1**, 3–5.
- K. Li, H.-R. Xu, K.-K. Yu, J.-T. Hou and X.-Q. Yu, *A coumarin-based chromogenic and ratiometric probe for hydrazine, Anal. Methods*, 2013, **5**, 2653–2656 (doi.org/10.1039/C3AY40148K).
- Y. D. Lin and T. J. Chow, *A pyridomethene-BF<sub>2</sub> complex-based chemosensor for detection of hydrazine, RSC Adv.*, 2013, **3**, 17924–17929 (doi.org/10.1039/C3RA42717J).

- 17 S. Goswami, S. Das, K. Aich, B. Pakhira, S. Panja, S. K. Mukherjee and S. Sarkar, A Chemodosimeter for the Ratiometric Detection of Hydrazine Based on Return of ESIPT and Its Application in Live-Cell Imaging, *Org. Lett.*, 2013, **15**, 5412–5415 (doi.org/10.1021/ol4026759).
- 18 S. Goswami, K. Aich, S. Das, S. B. Roy, B. Pakhira and S. Sarkar, A reaction based colorimetric as well as fluorescence 'turn on' probe for the rapid detection of hydrazine, *RSC Adv.*, 2014, **4**, 14210–14214 (doi.org/10.1039/C3RA46663A).
- 19 X.-Q. Zhan, J.-H. Yan, J.-H. Su, Y.-C. Wang, J. He, S.-Y. Wang, H. Zheng and J.-G. Xu, Thiospirolactone as a recognition site: Rhodamine B-based fluorescent probe for imaging hypochlorous acid generated in human neutrophil cells, *Sens. Actuators B*, 2010, **150**, 774–780 (doi.org/10.1016/j.snb.2010.07.057).
- 20 K. Dou, Q. Fu, G. Chen, F. Yu, Y. Liu, Z. Cao, G. L. Li, X. Zhao, L. Xia, L. X. Chen, H. Wang and J. M. You, A novel dual-ratiometric-response fluorescent probe for  $\text{SO}_2/\text{ClO}^-$  detection in cells and in vivo and its application in exploring the dichotomous role of  $\text{SO}_2$  under the  $\text{ClO}^-$  induced oxidative stress, *Biomaterials*, 2017, **133**, 82–93 (DOI: 10.1016/j.biomaterials.2017.04.024).
- 21 Q. Fu, G. Chen, Y. Liu, Z. Cao, X. Zhao, G. Li, F. Yu, L. Chen, H. Wang and J. You, In situ quantification and evaluation of  $\text{ClO}^-/\text{H}_2\text{S}$  homeostasis in inflammatory gastric tissue by applying a rationally designed dual-response fluorescence probe featuring a novel  $\text{H}^+$ -activated mechanism, *Analyst*, 2017, **142**, 1619–1627 (doi.org/10.1039/C7AN00244K).
- 22 X. Jing, F. Yu and L. Chen, Visualization of nitroxyl (HNO) in vivo via a lysosome-targetable near-infrared fluorescent probe, *Chem. Commun.*, 2014, **50**, 14253–14256 (doi.org/10.1039/C4CC07561G).
- 23 P. Liu, X. Jing, F. Yu, C. Lv and L. Chen, A near-infrared fluorescent probe for the selective detection of HNO in living cells and in vivo, *Analyst*, 2015, **140**, 4576–4583 (doi.org/10.1039/C5AN00759C).
- 24 S. Goswami, S. Das, K. Aich, P. K. Nandi, K. Ghoshal, C. K. Quah, M. Bhattacharyya, H.-K. Fun and H. A. A.-Aziz, A rhodamine-quinoline based chemodosimeter capable of recognising endogenous  $\text{OCl}^-$  in human blood cells, *RSC Adv.*, 2014, **4**, 24881–24886 (doi.org/10.1039/C4RA03200D).
- 25 S. Goswami, K. Aich, S. Das, B. Pakhira, K. Ghoshal, C. K. Quah, M. Bhattacharyya, H.-K. Fun and S. Sarkar, A Triphenyl Amine-Based Solvatofluorochromic Dye for the Selective and Ratiometric Sensing of  $\text{OCl}^-$  in Human Blood Cells, *Chem. Asian J.*, 2015, **10**, 694 – 700 (doi.org/10.1002/asia.201403234).
- 26 S. D. Hiremath, R. U. Gawas, D. Das, V. G. Naik, A. A. Bhosle, V. Priya Murali, K. Kumar Maiti, R. Acharya, M. Banerjee and A. Chatterjee, Phthalimide conjugation turns the AIE-active tetraphenylethylene unit non-emissive: its use in turn-on sensing of hydrazine in solution and the solid- and vapour-phase, *RSC Adv.*, 2021, **11**, 21269–21278 (doi.org/10.1039/D1RA03563K).
- 27 S. Saha, S. Das, O. Sarkar, A. Chattopadhyay, K. Rissanen and P. Sahoo, Introduction of a Luminescent Dye for the Selective and Ratiometric Sensing of Hydrazine in Insect Pollinated Cropland Flowers, *New J. Chem.*, 2021, **45**, 17095–17100 (doi.org/10.1039/D1NJ02661E).
- 28 C. Bao, S. Shao, H. Zhou and Y. Han, A new ESIPT-based fluorescent probe for the highly sensitive detection of amine vapors, *New J. Chem.*, 2021, **45**, 10735–10740 (doi.org/10.1039/D1NJ01826D).
- 29 Y. Zhou, T. Liu, S. Zheng, X. Wang, M. Zhang, M. Irfan, Y. Zhang, H. Wang and Z. Zeng, A highly selective visual paper-based detector for hydrazine and MCL luminogens based on fluorinated-pyrrole-functionalized triphenylamine, *New J. Chem.*, 2021, **45**, 20173–20180 (New J. Chem., 2021, **45**, 20173–20180).
- 30 J. Pan, J. Ma, H. Liu, Y. Zhang and L. Lu, The preparation of a special fluorescent probe with an aggregation-induced emission effect for detecting hydrazine in water, *New J. Chem.*, 2021, **45**, 21151–21159 (doi.org/10.1039/D1NJ03498G).
- 31 W. Zhang, W. Song and W. Lin, A novel ER-targeted two-photon fluorescent probe for monitoring abnormal concentrations of HClO in diabetic mice, *J. Mater. Chem. B*, 2021, **9**, 7381–7385 (doi.org/10.1039/D1TB01327K).
- 32 K. Dąbrowa, M. Lindner, A. T.-Gumkowska and J. Jurczak, Imino-thiolate-templated synthesis of a chloride-selective neutral macrocyclic host with a specific "turn-off-on" fluorescence response for hypochlorite ( $\text{ClO}^-$ ), *Org. Chem. Front.*, 2021, **8**, 5258–5264 (doi.org/10.1039/D1QO00504A).
- 33 K. Zhang, H. Wang, S. Cheng, C. Zhang, X. Zhai, X. Lin, H. Chen, R. Gao and W. Dong, A benzaldehyde-indole fused chromophore-based fluorescent probe for double-response to cyanide and hypochlorite in living cell, *Analyst*, 2021, **146**, 5658–5667 (doi.org/10.1039/D1AN01015H).
- 34 A. Poghosian, M. Weil, A. G. Cherstvy and M. J. Schöning, Electrical monitoring of polyelectrolyte multilayer formation by means of capacitive field-effect devices, *Anal Bioanal Chem*, 2013, **405**, 6425–6436 (DOI 10.1007/s00216-013-6951-9).
- 35 Maryam H. Abouzar, A. Poghosian, A. G. Cherstvy, A. M. Pedraza, S. Ingebrandt and M. J. Schöning, Label-free electrical detection of DNA by means of field-effect nanoplate capacitors: Experiments and modelling, *Phys. Status Solidi A*, 2012, **209**, 925–934 (DOI 10.1002/pssa.201100710).
- 36 K. Li, H.-R. Xu, K.-K. Yu, J.-T. Hou and X.-Q. Yu, A coumarin-based chromogenic and ratiometric probe for hydrazine, *Anal. Methods*, 2013, **5**, 2653–2656 (doi.org/10.1039/C3AY40148K).
- 37 Y. Sun, D. Zhao, S. Fan and L. Duan, A 4-hydroxynaphthalimide-derived ratiometric fluorescent probe for hydrazine and its in vivo applications, *Sens. Actuators, B*, 2015, **208**, 512–517 (doi.org/10.1016/j.snb.2014.11.057).
- 38 X. Xia, F. Zeng, P. Zhang, J. Lyu, Y. Huang and S. Wu, An ICT-based ratiometric fluorescent probe for hydrazine detection and its application in living cells and in vivo, *Sens. Actuators, B*, 2016, **227**, 411–418 (doi.org/10.1016/j.snb.2015.12.046).
- 39 H. Bhutani, S. Singh, S. Vir, K. K. Bhutani, R. Kumar, A. K. Chakraborti and K. C. Jindal, LC and LC-MS study of stress decomposition behaviour of isoniazid and establishment of validated stability-indicating assay method, *J. Pharm. Biomed. Anal.*, 2007, **43**, 1213–1220 (DOI: 10.1016/j.jpba.2006.10.013).
- 40 M. Sun, L. Bai and D. Q. Lui, A generic approach for the determination of trace hydrazine in drug substances using in situ derivatization-headspace GC-MS, *J. Pharm. Biomed. Anal.*, 2009, **49**, 529–533 (DOI: 10.1016/j.jpba.2008.11.009).
- 41 Y. Zhu, J. Zhang and S. Dong, Hydrazines probe of interaction of horseradish peroxidase with cryo-hydrogel, *Anal. Chim. Acta*, 1997, **353**, 45–52 (doi.org/10.1016/S0003-2670(97)00385-1).
- 42 J.-A. Oh, J.-H. Park and H.-S. Shin, Sensitive determination of hydrazine in water by gas chromatography-mass spectrometry after derivatization with ortho-phthalaldehyde, *Anal. Chim. Acta*, 2013, **769**, 79–83 (doi.org/10.1016/j.aca.2013.01.036).
- 43 X. Gu and J. P. Camden, Surface-Enhanced Raman Spectroscopy-Based Approach for Ultrasensitive and Selective Detection of Hydrazine, *Anal. Chem.*, 2015, **87**, 6460–6464 (doi.org/10.1021/acs.analchem.5b01566).
- 44 J. Liu, W. Zhou, T. You, F. Li, E. Wang and S. Dong, Detection of Hydrazine, Methylhydrazine, and Isoniazid by Capillary

- Electrophoresis with a Palladium-Modified Microdisk Array Electrode, *Anal. Chem.*, 1996, **68**, 3350–3353 (doi.org/10.1021/ac9604696).
- 45 X. Cheng, H. Jia, T. Long, J. Feng, J. Qin and Z. Li, A “turn-on” fluorescent probe for hypochlorous acid: convenient synthesis, good sensing performance, and a new design strategy by the removal of C[double bond, length as m-dash]N isomerization, *Chem. Commun.*, 2011, **47**, 11978–11980 (doi.org/10.1039/C1CC15214A).
- 46 D. Li, Y. Feng, J. Lin, M. Chen, S. Wang, X. Wang, H. Sheng, Z. Shao, M. Zhu and X. Meng, A mitochondria-targeted two-photon fluorescent probe for highly selective and rapid detection of hypochlorite and its bio-imaging in living cells, *Sens. Actuators, B*, 2016, **222**, 483–491.
- 47 X. Chen, K.-A. Lee, X. Ren, J.-C. Ryu, G. Kim, J.-H. Ryu, W.-J. Lee and J. Yoon, Synthesis of a highly HOCl-selective fluorescent probe and its use for imaging HOCl in cells and organisms, *Nat. Protoc.*, 2016, **11**, 1219–1228 (doi:10.1038/nprot.2016.062).
- 48 L. Cao, R. Zhang, W. Zhang, Z. Du, C. Liu, Z. Ye, B. Song and J. Yuan, A ruthenium(II) complex-based lysosome-targetable multisignal chemosensor for in vivo detection of hypochlorous acid, *Biomaterials*, 2015, **68**, 21–31 (doi.org/10.1016/j.biomaterials.2015.07.052).
- 49 L. Yuan, L. Wang, B. K. Agrawalla, S.-J. Park, H. Zhu, B. Sivaraman, J. Peng, Q.-H. Xu and Y.-T. Chang, Development of Targetable Two-Photon Fluorescent Probes to Image Hypochlorous Acid in Mitochondria and Lysosome in Live Cell and Inflamed Mouse Model, *J. Am. Chem. Soc.*, 2015, **137**, 5930–5938.
- 50 L. Wu, I. C. Wu, C. C. DuFort, M. A. Carlson, X. Wu, L. Chen, C.-T. Kuo, Y. Qin, J. Yu, S. R. Hingorani and D. T. Chiu, Photostable Ratiometric PdOT Probe for in Vitro and in Vivo Imaging of Hypochlorous Acid, *J. Am. Chem. Soc.*, 2017, **139**, 6911–6918 (doi.org/10.1021/jacs.7b01545).
- 51 S. Goswami, S. Das, K. Aich, D. Sarkar, T. K. Mondal, C. K. Quah, H. K. Fun, CHEF induced highly selective and sensitive turn-on fluorogenic and colorimetric sensor for Fe<sup>3+</sup>, *Dalton Transactions*, 2013, **42**, 15113–15119 (doi.org/10.1039/C3DT51974K).
- 52 S. Goswami, S. Das, K. Aich, An ICT based highly selective and sensitive sulfur-free sensor for naked eye as well as fluorogenic detection of Hg<sup>2+</sup> in mixed aqueous media, *Tetrahedron Lett.*, 2013, **54**, 4620–4623 (doi.org/10.1016/j.tetlet.2013.06.035).
- 53 S. Das, K. Aich, S. Goswami, C. K. Quah, H. K. Fun, FRET-based fluorescence ratiometric and colorimetric sensor to discriminate Fe<sup>3+</sup> from Fe<sup>2+</sup>, *New Journal of Chemistry*, 2016, **40**, 6414–6420 (doi.org/10.1039/C5NJ03598H).
- 54 S. Das, P. P. Das, J. W. Walton, K. Ghoshal, L. Patra, M. Bhattacharyya, FRET based ratiometric switch for selective sensing of Al<sup>3+</sup> with bio-imaging in human peripheral blood mononuclear cells, *New Journal of Chemistry*, 2021, **45**, 1853–1862 (doi.org/10.1039/D0NJ05546H).
- 55 S. Das, P. P. Das, J. W. Walton, K. Ghoshal, L. Patra and M. Bhattacharyya, An excited state intramolecular proton transfer induced phosphate ion targeted ratiometric fluorescent switch to monitor phosphate ions in human peripheral blood mononuclear cells, *Dalton Trans.*, 2022, **51**, 10779–10786 (doi.org/10.1039/D2DT00581F).
- 56 S. Das, K. Aich, L. Patra, K. Ghoshal, S. Gharami, M. Bhattacharyya, T. K. Mondal, Development of a new fluorescence ratiometric switch for endogenous hypochlorite detection in monocytes of diabetic subjects by dye release method, *Tetrahedron Lett.*, 2018, **59**, 1130–1135 (doi.org/10.1016/j.tetlet.2018.02.023).
- 57 K. Wang, G. Lai, Z. Li, M. Liu, Y. Shen, C. Wang, A novel colorimetric and fluorescent probe for the highly selective and sensitive detection of palladium based on Pd(0) mediated reaction, *Tetrahedron*, 2015, **71**, 7874–7878 (doi.org/10.1016/j.tet.2015.08.021).
- 58 M. Shortreed, R. Kopelman, M. Kuhn and B. Hoyland, Fluorescent fiber-optic calcium sensor for physiological measurements, *Anal. Chem.*, 1996, **68**, 1414 (DOI: 10.1021/ac950944k).
- 59 W. Lin, L. Yuan, Z. Cao, Y. Feng and L. Long, A Sensitive and Selective Fluorescent Thiol Probe in Water Based on the Conjugate 1, 4-Addition of Thiols to  $\alpha$ ,  $\beta$ -Unsaturated Ketones, *Chem. – Eur. J.*, 2009, **15**, 5096 (doi.org/10.1002/chem.200802751).
- 60 B. Valeur, *Molecular Fluorescence. Principles and Applications*; Wiley-VCH: Weinheim, Germany, 2002.
- 61 A. D. Becke, Density-functional thermochemistry. III. The role of exact exchange, *J. Chem. Phys.*, 1993, **98**, 5648–5652 (doi.org/10.1063/1.464913).
- 62 D. Andrae, U. Haeussermann, M. Dolg, H. Stoll and H. Preuss, Energy-adjusted *ab initio* pseudopotentials for the second and third row transition elements, *Theor. Chim. Acta*, 1990, **77**, 123–141 (doi.org/10.1007/BF01114537).